UDK 628.483:669-153
Original scientific article/Izvirni znanstveni članek

ISSN 1580-2949
MTAEC9, 57(2)111(2023)

CORROSION BEHAVIOUR OF ANNEALED 42CrMo4 STEEL

KOROZIJSKO OBNAŠANJE ŽARJENEGA JEKLA VRSTE 42CrMo4

Lovro Liverić[1*], Dario Iljkić[1], Zoran Jurković[1], Nikša Čatipović[2], Paweł Nuckowski[3], Oktawian Bialas[4]

[1]University of Rijeka, Faculty of Engineering, Vukovarska 58, 51000 Rijeka, Croatia
[2]University of Split, Faculty of Electrical Engineering, Mechanical Engineering and Naval Architecture, Ruđera Boškovića 32, 21000 Split, Croatia
[3]Materials Research Laboratory, Faculty of Mechanical Engineering, Silesian University of Technology, ul. Konarskiego 18a, Gliwice 44-100, Poland
[4]Department of Engineering Materials and Biomaterials, Faculty of Mechanical Engineering, Silesian University of Technology, ul. Konarskiego 18a, Gliwice 44-100, Poland

Prejem rokopisa – received: 2022-09-14; sprejem za objavo – accepted for publication: 2023-01-20

doi:10.17222/mit.2022.624

In this paper, the corrosion behaviour of 42CrMo4 low-alloy steel after normalizing, soft annealing, spheroidizing annealing and full annealing is investigated. 42CrMo4 is steel for quenching and tempering, and one of the widely used and studied steels due to its good combination of mechanical properties. Sometimes, it is used in the annealed condition. Nevertheless, the corrosion properties of 42CrMo4 steel are poorly studied, especially in the annealed condition. The main objective of this work is to increase the knowledge about the corrosion behaviour of the investigated alloy. The mechanical and microstructure properties of the samples after different annealing processes were characterised with hardness testing, optical and scanning electron microscopy (SEM) and X-ray diffraction (XRD). Measurements of the open-circuit potential and potentiodynamic polarisation of the samples after different annealing processes were carried out in a naturally aerated solution. It was found that the corrosion rate of the soft annealed samples was higher than that of the spherical and full annealed samples. Moreover, full annealing resulted in a significant improvement in the corrosion resistance.

Keywords: heat treatment, annealing, corrosion, 42CrMo4 steel, microstructure

V članku je opisano korozijsko obnašanje malo legiranega jekla 42CrMo4 po normalizaciji, mehkem žarjenju, sferoidizacijskem žarjenju in procesu popolne toplotne obdelave. Jeklo 42CrMo4 se po kaljenju in popuščanju zelo veliko uporablja zaradi dobre kombinacije mehanskih lastnosti, včasih se uporablja tudi v žarjenem stanju. V preteklosti so korozijske lastnosti tega jekla redko raziskovali, še posebej v žarjenem stanju. Glavni namen raziskave je bilo izboljšanje znanja o korozijskem obnašanju jekla 42CrMo4. Mehanske in mikrostrukturne lastnosti vzorcev preiskovanega jekla so določili s pomočjo merilnika trdote, optičnega in vrstičnega elektronskega mikroskopa (SEM) ter z rentgensko difrakcijo (XRD). Po različnih postopkih žarjenja vzorcev so s pomočjo potenciodinamične polarizacije in metode določitve potenciala odprtega tokokroga v naravno prezračeni raztopini določili njihovo odpornost proti koroziji. Na osnovi analiz so ugotovili, da je hitrost korozije mehko žarjenih vzorcev večja kot tistih, ki so bili sferoidizacijsko ali popolnoma odžarjeni. Poleg tega so ugotovili, da imajo popolnoma odžarjeni vzorci pomembno izboljšano korozijsko odpornost.

Ključne besede: toplotna obdelava, žarjenje, korozija, jeklo 42CrMo4, mikrostruktura

1 INTRODUCTION

Low-alloy 42CrMo4 steel (AISI 4140) is a medium carbon steel alloyed with chromium and molybdenum, often used for dynamic loads and in impact areas.[1] In a heat-treated condition, it offers various application possibilities such as high tensile strength and toughness. Steels with a medium carbon content between 0.30–0.55 % C and 0.60–1.65 % Mn are used when higher mechanical properties are desired. They are usually hardened and strengthened with heat treatment or cold working. This group of materials is widely used for certain types of cold-formed parts that require annealing, normalizing or quenching and tempering before use.[1–4] Steel 42CrMo4 is steel for quenching and tempering, and one of the widely used and studied steels due to its good combination of mechanical properties.[1] Sometimes, it is used in the annealed condition.

Normalizing is the heat treatment performed by austenitizing and air cooling to produce a uniform, fine ferrite/pearlite microstructure in steel. The higher austenitizing temperatures used in normalizing ensure that most carbides are dissolved. Upon cooling, the austenite transforms into a coarse, non-uniform ferrite/pearlite microstructure. This microstructure provides an excellent starting point for subsequent hardening heat treatments.[5,6]

Heat treatments that produce microstructures consisting of spherical carbide particles, uniformly distributed in a ferrite matrix are called spheroidizing or spheroidizing annealing heat treatments. Spheroidized microstructures are the most stable microstructures found in steels, formed in any structure heated at sufficiently high temperatures and for sufficiently long times to allow diffusion-dependent nucleation and growth of spherical parti-

*Corresponding author's e-mail:
lliveric@riteh.hr (Lovro Liverić)

Table 1: Chemical composition of 42CrMo4 steel (balance Fe)

Chemical composition, *w*/%											
C	Si	Mn	P	S	Ni	Cr	Mo	Cu	Al	Ti	V
0.427	0.214	0.846	0.0056	0.0173	0.0407	1.07	0.183	0.167	0.0386	0.0089	0.0106

cles. Therefore, there are many different heat treatment processes for producing spheroidized microstructures.[6,7] There are two stages of the microstructural change associated with the formation of a spheroidized microstructure. The first stage is the formation of spherical carbide particles from other microstructures. A common starting point is pearlite, where cementite is present in essentially plate-like lamellae with a very large interfacial area per unit volume. The initial spherical microstructures consist of highly dense, very fine particles. Therefore, the second stage of spheroidization begins when the fine particles with small radii of the curvature dissolve and coarse particles grow, presenting in turn an interfacial energy-reduction mechanism. Diffusion-dependent spheroidization can take many hours depending on the alloy content, spheroidizing temperature and the degree of coarsening required. The slowest spheroidization is associated with coarse pearlitic microstructures. Many other methods of spheroidization are used to speed up the process.[6,7]

Soft annealing and spheroidize annealing have essentially the same process mechanism for producing spheroidized microstructures, but with the main difference being the cooling time. In the case of soft annealing, the cooling in air is slow, while in the case of spheroidize annealing, the cooling in a furnace is much slower.[1–7]

Full annealing can be described as a process, in which steels are heated to just above the A_{C3} temperature for low and medium carbon steels and then slowly cooled in furnaces after the heating is complete. The slow cooling causes an austenite transformation into ferrite and pearlite near the A_{C3} and A_{C1} temperatures, respectively, and ensures that coarse-grained equiaxed ferrite and pearlite with coarse interlamellar spacing form, resulting in a microstructure with high ductility and moderate strength. Once the austenite has transformed into ferrite and pearlite, the cooling rate can be increased to reduce the processing time and thus increase productivity. Although ferrite and pearlite microstructures are most often formed with full annealing at the above temperatures, microstructures of spheroidized carbide particles can sometimes also form in ferrite.[6,7]

Although the main purpose of heat treatment is to change the mechanical properties,[8–13] heat treatment also changes the corrosion properties of a material.[14,15]

Electrochemical corrosion is a destructive attack on a metallic material via an electrochemical reaction with the environment that negatively affects the critical mechanical properties of components. Seawater is a nearly universal fluid for evaluating the corrosion resistance of metallic materials.[1–4,7–17] Any material that exhibits good corrosion resistance in seawater is considered satisfactory for important aqueous applications.[9–17] Corrosion is affected by external and internal factors. External factors are corrosive medium parameters such as corrosive medium composition, pH, temperature and velocity, while internal factors are material parameters.[8–11]

Microstructural constituents are the most important material parameters that can affect the corrosion resistance of steels. A heterogeneous ferrite-pearlite microstructure of annealed steel forms anodic and cathodic sites that lead to corrosion. Alloy additions of less than 5 % have little effect on corrosion by seawater.[13,14,17]

In this work, the corrosion behaviour of 42CrMo4 steel subjected to different annealing processes was studied. The aim of this work was to increase the knowledge about the corrosion resistance of 42CrMo4 steel after normalizing (N), soft annealing (A), spheroidizing (AC) and full annealing (fA). The main objective was to investigate which process of the previously mentioned heat treatments exhibits the best corrosion resistance of annealed 42CrMo4 steel.

For this purpose, chemical composition, microstructural characterization and electrochemical studies were carried out. The chemical composition was determined using a glow discharge optical emission spectrometer (GDOES). The microstructure was studied with optical and electron microscopy. A phase analysis was performed using an X-ray diffractometer. Measurements of the open-circuit potential and potentiodynamic polarization of the annealed samples were performed using a computer-controlled potentiostat with three electrodes in a 0.6 M NaCl naturally aerated solution.

2 EXPERIMENTAL PART

2.1 Materials

Investigated samples were prepared by cutting manufactured ø16 mm steel bars of normalized 42CrMo4 steel into smaller pieces measuring 4 mm in length. An LECO GDS 500 A glow discharge optical emission spectrometer was used to determine the chemical composition of steel (**Table 1**).

2.2 Heat treatment

The thermal processes applied in this research are schematically compared in **Figure 1**. The heat treatment parameters are shown in **Table 2**.

The heat treatment parameters performed on the samples are shown in **Table 2**. The A_{C3} temperature is 790 °C, while A_{C1} is 745°C. The cooling rate and temperatures of the processes made the difference in the

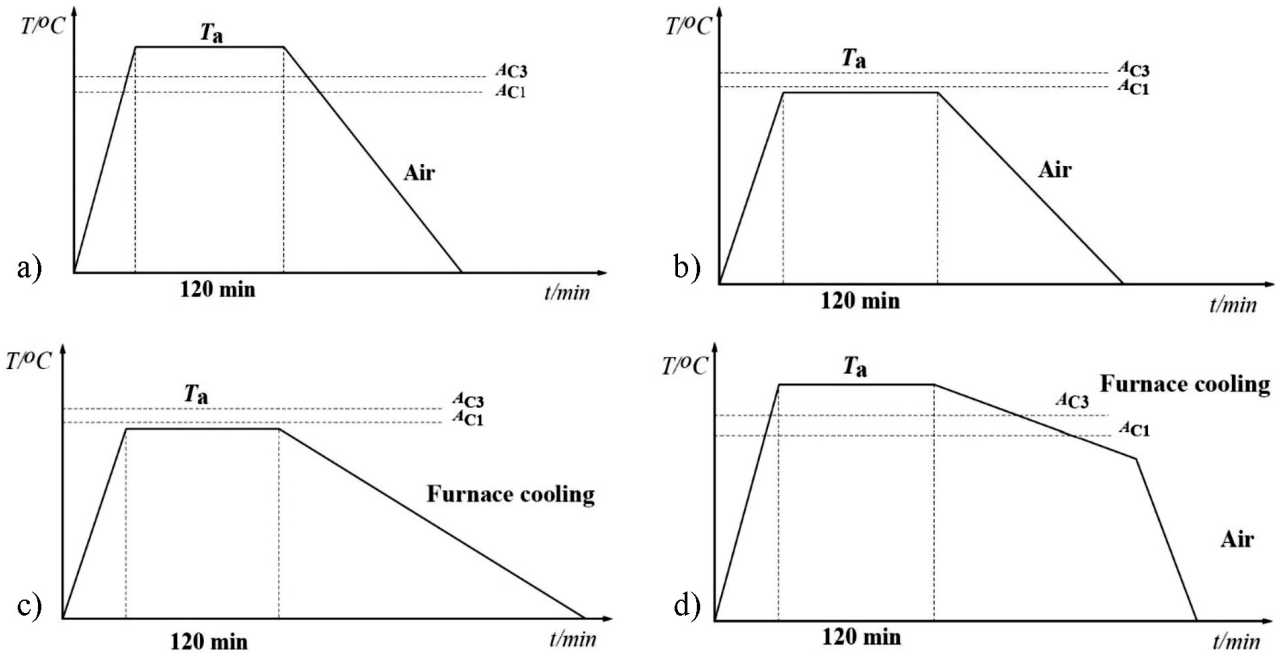

Figure 1: Thermal processes: a) normalizing (N), b) soft annealing (A), c) spheroidizing (AC) and d) full annealing (fA)

Table 2: Heat treatment parameters

Sample No:	Heat treatment	Parameters			Hardness
		Temperature	Time	Cooling medium	
1	Normalizing (N)	870 °C	120 min	Air	90 HRB ±3 HRB
2	Soft annealing (A)	720 °C	120 min	Air	90 HRB ±3 HRB
3	Spheroidizing annealing (AC)	735 °C	120 min	Furnace cooling	89 HRB ±3 HRB
4	Full annealing (fA)	820 °C	120 min	From 820 °C furnace cooling to 670°C, then air	75 HRB ±3 HRB

microstructure that is later observed. Normalization consisted of heating beyond the A_{c3} temperature and slow air-cooling after a similar holding time. A similar treatment with heating beyond the A_{c3} temperature is full annealing, using a slightly lower temperature in comparison to normalization, and then cooling below the A_{c1} temperature. The cooling consisted of very slow furnace cooling, fallowed by air cooling from a certain point. With that combination of cooling, the microstructure changed, resulting in a drop in the hardness. Comparing the soft and spheroidizing annealing process, we find that the holding temperature of annealing was nearly the same, but a big difference was distinguished between the cooling processes. Soft-annealing cooling included air-cooling of the samples to room temperature, while in spheroidising, the cooling process took place in the furnace and was way slower then air cooling. In this process, the microstructure change reflected on the mechanical and corrosion properties of the material. However, the hardness was not the best example for comparing the two methods.

2.3 Hardness test

The hardness after the heat treatment processes was measured for the purpose of checking the processes. The hardness of the specimens was measured using a ZHU 187.5 universal hardness tester with a Rockwell B (HRB) hardness 1.588 mm diameter steel carbide ball indenter. Before the measurements, the carburized layer was removed. The hardness results in **Table 2** are given in average values of five measurements with the standard deviation. The hardness values obtained after the annealing processes are in accordance with experimental literature data.[8] The results show that samples 1, 2 and 3 have similar hardness values, while sample 4 shows a lower value.

2.4 Microstructure characterization

The importance of microstructure for the properties of metal materials has long been recognized. Therefore, a microstructural characterization was done after the annealing processes to understand the connection between the microstructure and corrosion resistance of 42CrMo4 steel. The microstructure of annealed samples was observed using an Axio Vert A1 light Zeiss microscope with an AxioCam ERc 5s microscope module and a FEG QUANTA 250 SEM FEI scanning electron microscope with an EDS OXFORD detector.

Metallographic samples were prepared by grinding and polishing them with a STRUERS LABOPOL device,

grinding on an MD-Piano 220 resin bonded diamond disc, followed by using an MD-Allegro composite disc with different diamond suspensions. The samples were polished with an MD-Dac polishing cloth with DiaPro Dac 3- and 1-micron diamond suspension, followed by an MD-Chem polishing cloth with OP-U NonDry colloidal silica suspension. The samples were etched using Nital 3 % solution for 10–20 s.

X-ray diffraction was carried out on a PANalytical X'Pert Pro MPD diffractometer, with the use of filtered X-ray lamp radiation (Fe filter) with a cobalt anode (K Co_α = 0.17909 nm), powered by a voltage of 40 kV and with a filament current intensity of 30 mA. X-ray diffraction measurements were performed in the Bragg-Brentano geometry in an angular scope of 20–120° [2θ] with a step of 0.05° and a step count time of 100 s. The obtained diffractograms were analysed by means of the X'Pert HighScore Plus software (v. 3.0e) with a dedicated Inorganic Crystal Structure Database – ICSD (FIZ, Karlsruhe, Germany).

2.5 Electrochemical corrosion behaviour

Electrochemical investigations were performed using a computer-controlled Princeton Applied Research potentiostat, Parstat 2263. A three-electrode set-up was used: the working electrode with an exposed area of 1 cm^2, a saturated calomel electrode (SCE) placed in a Luggin capillary as the reference electrode and the graphite counter electrode. Before the electrochemical investigations, the samples were ground with the P320, P600, P800, P1200 and P2400 sandpapers, then degreased in ethanol and rinsed with deionized water. All the measurements were conducted at room temperature (20 ± 2 °C), in a 0.6 M NaCl naturally aerated solution, prepared from analytical grade NaCl and deionized water. Open circuit potential, E_{OC}, measurements were performed as a function of time for a period of 2 h. Potentiodynamic polarization was performed at a scan rate of 0.166 mVs^{-1}, over a potential range of E_{OC} ± 250 mV, starting from the most negative potential. The corrosion rate was calculated from polarization curves, based on the corrosion current density, i_{corr}, known equivalent weight (EW = 28.558 g) and density (ρ = 7.85 gcm^{-3}) of 42CrMo4 steel, in accordance with the expression:

$$v_{corr} = \frac{0.0033 \cdot i_{corr} \cdot EW}{\rho} \quad (1)$$

3 RESULTS AND DISCUSSION

Figure 2 shows the microstructures of 42CrMo4 steel after different annealing processes taken with the optical microscope with 200× magnification lens. The heterogeneous microstructure of the normalized 42CrMo4 steel comprised of ferrite crystals among the colonies of pearlite is shown in **Figure 2a**. The microstructures of

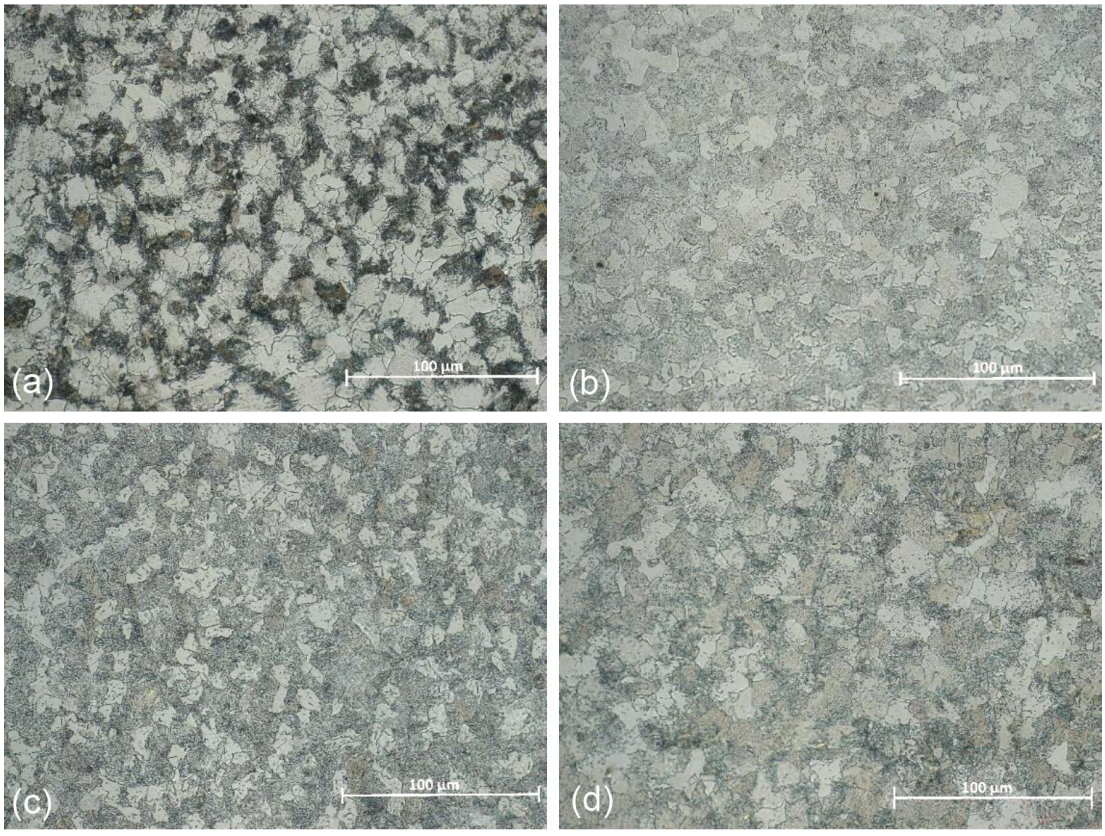

Figure 2: Optical-microscope micrographs of annealed samples: a) Sample 1 (N), b) Sample 2 (A), c) Sample 3 (AC), d) Sample 4 (fA)

the samples contain distinguished pearlite and ferrite phases. The annealing process produced uniformly distributed pearlite in the matrix of ferrite, with pearlite in larger fractions as previously reported by Lu et al.[15] Pearlite is dark and ferrite is light. The ratio of the pearlite/ferrite phases depends mainly on the chemical composition (% C) and heat treatment parameters where the cooling rate is critical.

The observed and compared microstructures are generally similar. They consist of pearlite randomly distributed in the matrix of ferrite, with differences in the grain size. Comparing the microstructures of differently heat-treated samples, we can see the influence of different cooling rates on diffusion-dependent nucleation and growth of spherical cementite particles in pearlite. In Sample 2 (**Figure 2b**), we can see the beginning of the second stage of spheroidization when the fine particles with small radii of curvature dissolve and coarse particles grow. While the micrographs from **Figure 2** were obtained with optical microscopy, **Figure 3** shows scanning-electron micrographs.

SEM images also show that the samples have similar grain and boundary structures, but differ in the ratio of the phases. The largest grain size is found in the normalized sample, Sample 1 (**Figure 3a**), while the smallest grain size and the largest number of grains are found in the spheroidized annealed sample, Sample 3 (**Figure 3c**). The fully annealed sample (**Figure 3d**) shows the biggest amount of precipitation in the microstructure.

To simplify the estimation of the relative amounts of the phases present and to identify the phases, the relative intensity from the XRD results is given, on a scale, in **Figure 4**. The following phases are indexed on the figure: # – α iron (α-Fe), * – cementite (Fe_3C). The patterns

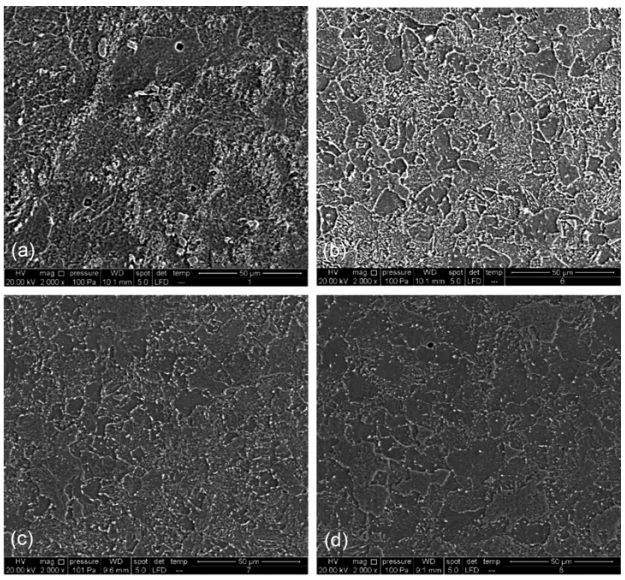

Figure 3: SEM, LFD micrographs of annealed-sample microstructures: a) Sample 1 (N), b) Sample 2 (A), c) Sample 3 (AC), d) Sample 4 (fA)

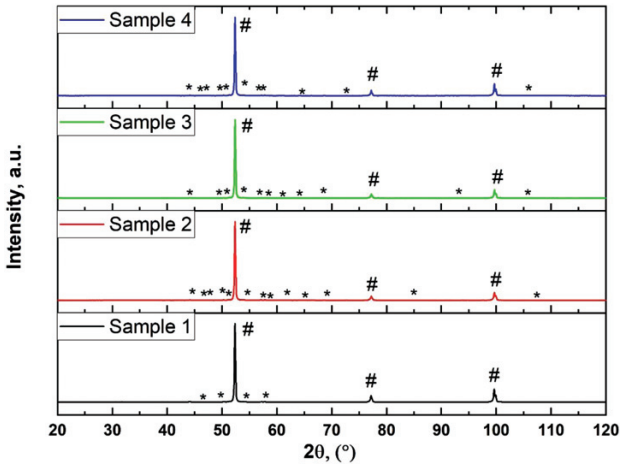

Figure 4: XRD patterns of samples: a) Sample 1 (N), b) Sample 2 (A), c) Sample 3 (AC), d) Sample 4 (fA)

are given in the units of reticular distances. All the samples have the iron alpha phase (α-Fe), known as ferrite, and cementite (Fe_3C). As can be seen from the distribution of the phases in **Figure 4**, the densities of the phases in the structure are similar. General differences can be seen in the distribution of cementite, which is due to different cooling rates of the samples during heat treatment.

Potentiodynamic polarization curves presented with a semi-logarithmic plot (**Figure 5**) are composed of cathodic and anodic branches, resulting from the electrochemical reactions in the system. The anodic branch of a polarization curve describes the anodic dissolution of iron in the NaCl solution, while the cathodic part of the polarization curve represents the oxygen reduction reaction. Compared to normalized steel (Sample 1), whose state is solid on a large scale, annealed Samples 2 and 3 have an anodic current density that increases much faster with the potential, indicating active dissolution, while the cathodic current density increases much slower, being characteristic of a diffusion-controlled process, which is

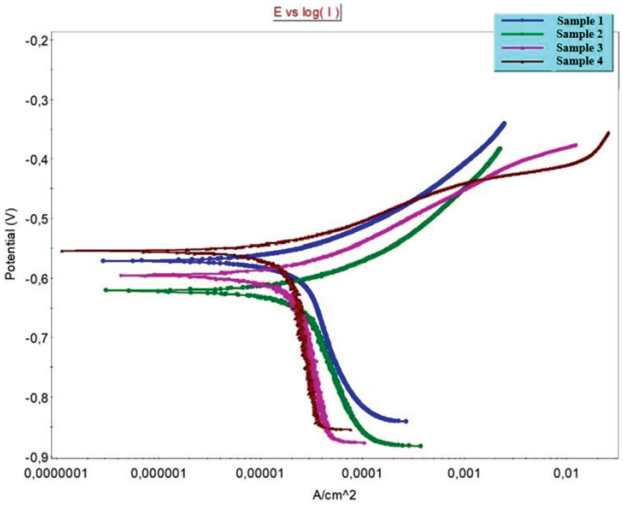

Figure 5: Potentiodynamic polarization curves for samples in 0.6 M NaCl solution: a) Sample 1 (N), b) Sample 2 (A), c) Sample 3 (AC), d) Sample 4 (fA)

Table 3: Corrosion parameters of the samples taken from potentiodynamic polarization curves

Sample No.	E_{corr}	i_{corr}	β_c[1]	β_a[2]	v_{corr}	Potential range
	(mV)	(μA cm^{-2})	(mV dec^{-1})	(mV dec^{-1})	(mmpy)	(mV)
1.	–570.90	41.72	–1009.339	119.967	0.32240	–841, –341
2.	–621.26	52.72	–1591.233	134.522	0.40740	–882, –382
3.	–595.95	26.91	–1327.532	89.908	0.20800	–876, –376
4.	–554.07	20.52	–1254.861	66.100	0.15860	–836, –412

[1] cathodic Tafel slope; [2] anodic Tafel slope

reversed compared to Sample 4 as it is similar to the normalized sample.[14,15] It can be seen that the values of the anodic current, i_a, are much higher than those of the cathodic current, i_c, at high overvoltage values. This indicates that the reduction process is slower than the oxidation process so that the cathodic reaction controls the electrochemical corrosion of 42CrMo4 steel.

Corrosion parameters obtained from the polarization measurements are shown in **Table 3**. All the tested samples have a low corrosion current density, i_{corr}, indicating a low corrosion rate, v_{corr}. When comparing Sample 1 and annealed Sample 2, they show similar corrosion rates, while the corrosion rates of Samples 3 and 4 are up to twice lower. Similar observations for annealed 42CrMo4 steel was found in the literature.[1–4,9–17] The corrosion resistance of the samples can be explained with the density ratio of the pearlite phase and with the grain size of the pearlite/ferrite structure. As seen in **Figures 2 and 3**, the grain size and density ratio of the pearlite phase in the microstructure are similar in Samples 1 and 2, and in Samples 3 and 4.

Among the annealed samples, Sample 4 had the corrosion rate lower than 0.16 mmpy, which was consistently obtained for full annealing at 820 °C for 120 min, followed by very slow furnace cooling from 820 °C to 670 °C and air cooling to room temperature.

Moreover, this sample showed a pronounced corrosion-potential shift in the positive direction upon heat treatment. Overall, all the samples have low corrosion rates, which may indicate the influence of surface passivation due to the presence of chromium and molybdenum in the steel.[1,10] Another reason may be the effect of the spheroidization process on the coarsening and spheroidization of cementite that are more pronounced at a slower cooling time, leading to a smaller cathodic reactivity and to a reduction in the cementite-to-ferrite area. It can be concluded that the influences of the grain size, density ratio of the pearlite phase and ratio of the pearlite/ferrite structure of the annealed 42CrMo4 steel can influence the corrosion resistance, especially after a longer cooling time after heat treatment.

5 CONCLUSIONS

The corrosion behaviour of low-alloy 42CrMo4 steel after different annealing processes was analysed with potentiodynamic polarization. In addition, the electrochemical corrosion behaviour was examined with a hardness test, optical and electron microscopy and XRD analyses. The following conclusions can be drawn:

- Annealed 42CrMo4 steel samples have similar hardness values, characteristic for annealed steel.
- The observed morphology of the annealed samples shows a uniform arrangement of pearlite and ferrite phases. Soft and spheroidized annealed samples show different stages of the spheroidization of the pearlite phases.
- XRD results show that the structures of the annealed samples consist of the iron alpha phase (α-Fe), known as ferrite, and the cementite phase (Fe_3C). Moreover, XRD results show that the distributions and densities of the phases in the structures are similar.
- The parameters of the annealing process influence the corrosion behaviour of 42CrMo4 steel. The fully annealed 42CrMo4 steel sample exhibits the best corrosion resistance, while the soft annealed 42CrMo4 steel sample exhibits the lowest corrosion resistance.
- The differences between the sample results can be explained with the effects on the coarsening and spheroidization of cementite, which are more pronounced at slower cooling, leading to a smaller cathodic reactivity and a reduction in the cementite-to-ferrite area.

Acknowledgment

This work has been supported in part by University of Rijeka under the project number uniri-tehnic-18-293.

6 REFERENCES

[1] S. Smokvina Hanza, L. Štic, L. Liverić, V. Špada, Corrosion behaviour of tempered 42CrMo4 steel, Mater. Tehnol., 55 (**2021**) 3, doi:10.17222/mit.2021.014

[2] G. Krauss, Steels: Heat Treatment and Processing Principles, ASM International, 1990

[3] Y. Totik, The Corrosion Behavior of AISI 4140 Steel Subjected to Different Heat Treatments, Corrosion Reviews, 23 (**2005**) 4–6, 379–390, doi:10.1515/corrrev.2005.23.4-5-6.379

[4] Y. Totik, The corrosion behaviour of manganese phosphate coatings applied to AISI 4140 steel subjected to different heat treatments, Surface and Coatings Technology, 200 (**2006**) 8, 2711–2717, doi:10.1016/j.surfcoat.2004.10.004

[5] G. E. Totten, Steel Heat Treatment: Metallurgy and Technologies, 2nd ed., CRC Press, Taylor & Francis Group, 2007

[6] G. Krauss, Steels: Processing, structure, and performance, ASM International, 2016

[7] K. E. Thelning, Steel and its heat treatment, Butterworths, 1984

[8] M. Fattah, F. Mahboubi, Microstructure Characterization and Corrosion Properties of Nitrocarburized AISI 4140 Low Alloy Steel, Journal of Materials Engineering and Performance, 21 (**2011**) 4, 548–552, doi:10.1007/s11665-011-9922-3

[9] M. Khani Sanij, S. Ghasemi Banadkouki, A. Mashreghi, M. Moshrefifar, The effect of single and double quenching and tempering heat treatments on the microstructure and mechanical properties of AISI 4140 steel, Materials and Design, 42 (**2012**), 339–346, doi:10.1016/j.matdes.2012.06.017

[10] P. Katiyar, S. Misra, K. Mondal, Corrosion Behavior of Annealed Steels with Different Carbon Contents (0.002, 0.17, 0.43 and 0.7% C) in Freely Aerated 3.5% NaCl Solution, Journal of Materials Engineering and Performance, 28 (**2019**) 7, 4041–4052, doi:10.1007/s11665-019-04137-5

[11] M. Hafeez, A. Farooq, Effect of Heat Treatments on the Mechanical and Electrochemical Corrosion Behavior of 38CrSi and AISI 4140 Steels, Metallography, Microstructure, and Analysis, 8 (**2019**) 4, 479–487, doi:10.1007/s13632-019-00556-x

[12] M. Szala, G. Winiarski, Ł. Wójcik, T. Bulzak, Effect of Annealing Time and Temperature Parameters on the Microstructure, Hardness, and Strain-Hardening Coefficients of 42CrMo4 Steel, Materials, 13 (**2020**) 9, 2022, doi:10.3390/ma13092022

[13] A. Çalık, O. Dokuzlar, N. Uçar, The effect of heat treatment on mechanical properties of 42CrMo4 steel, Journal of Achievements in Materials and Manufacturing Engineering, 1 (**2020**) 98, 5–10, doi:10.5604/01.3001.0014.0811

[14] F. Sarıoğlu, The effect of tempering on susceptibility to stress corrosion cracking of AISI 4140 steel in 33% sodium hydroxide at 80°C, Materials Science and Engineering: A, 315 (**2001**) 1–2, 98–102, doi:10.1016/s0921-5093(01)01198-4

[15] F. Zhu, X. Luo, F. Chai, C. Yang, Z. Zhang, Effect of double quenching process and tempering temperature on the microstructure and mechanical properties of a High Strength Low Alloy Steel, IOP Conference Series: Materials Science and Engineering, 772 (**2020**) 1, 012010, doi:10.1088/1757-899x/772/1/012010

[16] Surface Morphology of Metal Electrodeposits, In: Fundamental Aspects of Electrometallurgy, Springer, Boston, MA, 2002, doi:10.1007/0-306-47564-2_3

[17] J. Wei, Y. Zhou, J. Dong, X. He, W. Ke, Effect of cementite spheroidization on improving corrosion resistance of pearlitic steel under simulated bottom plate environment of cargo oil tank, Materialia, 6 (**2019**), 100316, doi:10.1016/j.mtla.2019.100316